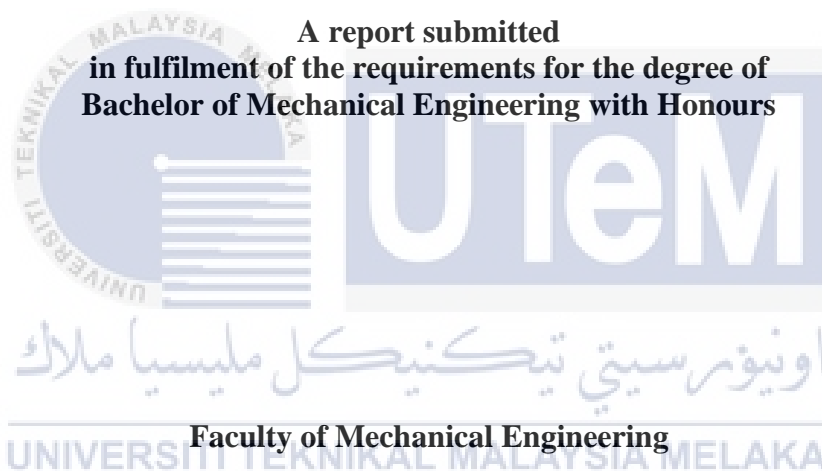


**Crashworthiness Finite Element Analysis on Aluminium Alloy Shells
Under Quasi-Static Axial Loading**

LEE JIN DE



UNIVERSITI TEKNIKAL MALAYSIA MELAKA

2021

DECLARATION

I declare that this project report entitled “Crashworthiness Finite Element Analysis on Aluminium Alloy Shells Under Quasi-Static Axial Loading” is the result of my own work except as cited in the references.



Signature	:
Name	:
Date	:

اونيورسيتي تيكنيكل مليسيا ملاك

UNIVERSITI TEKNIKAL MALAYSIA MELAKA

APPROVAL

I hereby declare that I have read this project report and in my opinion this report is sufficient in terms of scope and quality for the award of the degree of Bachelor of Mechanical Engineering with Honours.



Signature :

Supervisor's Name :

Date :

اونيورسيتي تيكنيكل مليسيا ملاك

UNIVERSITI TEKNIKAL MALAYSIA MELAKA

ABSTRACT

Thin-walled shells are used as energy absorbers due to its weight efficiency and its ability to absorb energy. The crashworthiness of the shells can be evaluated by comparing the crash parameters such as energy absorption capacity and initial peak crushing force. The cross-sectional geometry of the shells has played the main role in the variation of these crash parameters. Cylindrical shell which has the highest energy absorption had experienced the highest amount of initial peak crushing force which reduced its crashworthiness. Hence, investigate the deformation behaviour of shells with different cross-sectional geometry and its respective energy absorption ability and the effect of the hole on the crashworthiness of the thin-walled shell is the further aim of this study. The analysis starts up with three cross-sectional thin-walled shells which are circular, squarical, and triangular. The model is verified by comparing the numerical and the theoretical mean crushing force and their respective crash parameter is determined to identify the shell with the highest energy absorbed. The selected shell is modified to improve its crashworthiness by cutting out a hole on the shell. There is a total of 6 models with holes. There are 3 models with one hole on one side of the shell and 3 models with two holes on two sides of the shell. The hole is located at 20mm from the top of the shell to the centre of the hole, 20mm from the bottom of the shell to the centre of the hole, and at the middle height of the shell. All the model is assigned with Aluminium Alloy 6061, and it is subjected to 5mm/min quasi-static axial loading. The results found that cutting out hole was able to improve the crashworthiness of the shell.

ABSTRAK

Cangkang berding nipis digunakan sebagai penyerap tenaga kerana kecekapan berat dan kemampuannya untuk menyerap tenaga. Crashworthiness cangkang dapat dinilai dengan membandingkan parameter crash seperti kapasiti penyerapan tenaga dan daya penghancur puncak awal. Geometri keratan rentas cangkang telah memainkan peranan utama dalam variasi parameter ini. Cangkang silinder yang mempunyai penyerapan tenaga tertinggi mengalami jumlah daya penghancur puncak awal yang paling tinggi telah menyebabkan crashworthinya menurun. Oleh itu, selidiki tingkah laku ubah bentuk cangkang dengan geometri keratan rentas yang berbeza dan keupayaan penyerapan tenaga masing-masing dan kesan lubang pada kelayakan kerang dinding berding nipis adalah tujuan selanjutnya kajian ini. Analisis dimulakan dengan tiga cangkang berding nipis keratan rentas yang berbentuk bulat, segi empat, dan segitiga. Model-model ini diverifikasikan dengan membandingkan daya crash min berangka dan teoritis dan parameter crash masing-masing ditentukan untuk mengenalpasti cangkang yang kapasiti penyerapan tenaga tertinggi. Cangkang ini akan dipilih dan diubahsuaikan untuk meningkatkan crashworthiness-nya dengan memotong lubang pada cangkang. Terdapat sejumlah 6 model dengan lubang. Terdapat 3 model dengan satu lubang di satu sisi cangkang dan 3 model dengan dua lubang di dua sisi cangkang. Lubang terletak pada jarak 20mm dari bahagian atas cangkang ke pusat lubang, 20mm dari bahagian bawah cangkang ke pusat lubang, dan pada ketinggian tengah cangkang. Semua model dibuat daripada Aluminium Alloy 6061, dan dikenakan beban paksi separa-statik 5mm/min. Hasil kajian mendapati bahawa memotong lubang pada cangkang dapat meningkatkan crashworthiness cangkang.

ACKNOWLEDGEMENTS

First and foremost, I would like to take this opportunity to express my sincere acknowledgement to my supervisor Prof. Madya Ir. Dr. Sivakumar A/L Dhar Malingam from the Faculty of Mechanical Engineering Universiti Teknikal Malaysia Melaka (UTeM) for his essential supervision, support, and encouragement towards the completion of this project report. Also, appreciated his guide and comment on my work for me to improve better.

Thank you, to all my friend for their motivation and especially to who had guided me on using ABAQUS software which helped me reduce struggle time on the software. Besides, I would like to appreciate my parents for their moral support and motivation in completing this project. Lastly but not least, thank you to everyone who had been to the crucial parts of the realization of this research.

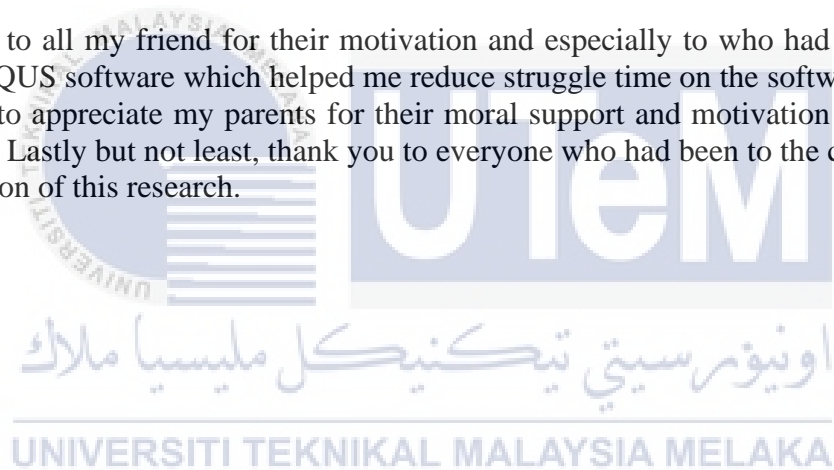


TABLE OF CONTENTS

	PAGES
DECLARATION	
ABSTRACT	i
ABSTRAK	ii
ACKNOWLEDGEMENTS	iii
TABLE OF CONTENTS	iv
LIST OF FIGURE	vi
LIST OF TABLE	xi
LIST OF ABBREVIATION	xiii
LIST OF SYMBOL	xiv
CHAPTER	
1. INTRODUCTION	1
1.1 Background	1
1.2 Problem statement	2
1.3 Objectives	2
1.4 Scope	2
2. LITERATURE REVIEW	3
2.1 Introduction	3
2.2 Thin-walled structures	3
2.3 Crash Parameter	5
2.3.1 Energy Absorption (EA)	6
2.3.2 Mean crush force (F_{mean})	6
2.3.3 Peak crush force (F_{max})	6
2.3.4 Crush force efficiency (CFE)	7
2.3.5 Specific Energy Absorption (SEA)	7
2.3.6 Crushing Strain	8
2.4 Axial loading on thin-walled structures	8
2.4.1 Effect of geometry on crashworthiness	14
2.4.2 Effect of material properties on crashworthiness	33
2.5 Hole Effect	42
2.6 Deformation mode	58
2.7 SUMMARY	68
3. METHODOLOGY	69
3.1 Introduction	69
3.2 CAD Geometry	70
3.3 Finite element analysis (FEA) setup	72
3.3.1 Boundary condition	72
3.3.2 Material	73
3.4 Meshing	74
3.5 Simulation validation	74
3.6 Numerical result	74

3.7	Analytical analysis	74
4.	RESULTS AND DISCUSSION	76
4.1	Quasi-static loading	76
4.2	Mesh Convergence Analysis	77
4.3	Numerical Results	78
4.4	Validation of numerical results	80
4.5	Energy absorbed and specific energy absorption	80
4.6	Peak crushing force	82
4.7	Crushing force efficiency and crushing strain	82
4.8	Modification with hole	83
4.9	Comparison of the crashworthiness of the shells	87
5.	CONCLUSION	93
5.1	Summary of Research	93
5.2	Suggestion For Future Work	94
	REFERENCES	95



LIST OF FIGURES

FIGURE	TITLE	PAGE
2.1	Axial crushing behaviour of the high-strength steel tubes with different impact mass.	9
2.2	Axial crushing behaviour of the high-strength steel tubes with different impact velocities.	10
2.3	Energy absorption capacity of the mild steel and high-strength steel tubes under various impact velocities .	11
2.4	50.8mm Al tube (a) As received (b) Annealed and (c) With eccentricity in thickness around tube circumference .	12
2.5	Comparison of experimental and numerical force-displacement curve .	13
2.6	50.8mm diameter Aluminium Tubes with (a) 50mm axial deformation, experimental (b) 50mm deformation full 360 degree FEA model (c) 60mm deformation with 9 degree reduced sector FE model .	13
2.7	Comparison of energy absorption capacity of different sections in experiments and numerical simulations for 1.5mm thickness tube .	15
2.8	Comparison of energy absorption capacity of different sections in experiments and numerical simulations for 1mm thickness tube .	15
2.9	Comparison of the maximum and the average force of various sections with 1.5 mm thickness from the experiment .	16
2.1	Basic collapse elements: (a) Type I; (b) type II.	17
2.11	Finite element solution for second buckling length.	17
2.12	Comparison of mean crush force diagram of all specimens.	19
2.13	Comparison of CFE of all specimens.	20

2.14	Comparison of crushing strain of all specimens.	20
2.15	Comparison of energy absorbed by all the specimens.	21
2.16	Comparison of the CFE for different cross-sectional geometry.	26
2.17	Comparison of the CS for different cross-sectional geometry.	27
2.18	Preparation of the square specimen.	29
2.19	Numerical model of the tube and jaws.	29
2.2	Cross-section geometry of the specimen and their respective dimension in mm. (a) Tr, (b) Tr-mc-1, (c) Tr mc-2, (d) Sq, (e) Sq-mc-1, (f) Sq-mc-2, (g) Hx, (h) Hx-mc-1, (i) Hx-mc-2, (j) Oc, (k) Oc-mc-1 and (l) Oc-mc-2.	30
2.21	Deformation behaviour of the samples (experiments). (a) Tr, (b) Tr-mc-1, (c) Tr-mc-2, (d) Sq, (e) Sq-mc-1, (f) Sq-mc-2, (g) Hx, (h) Hx-mc-1, (i) Hx-mc-2, (j) Oc, (k) Oc-mc-1 and (l) Oc-mc-2.	31
2.22	Deformation behaviour of the samples (simulation). (a) Tr, (b) Tr-mc-1, (c) Tr-mc-2, (d) Sq, (e) Sq-mc-1, (f) Sq-mc-2, (g) Hx, (h) Hx-mc-1, (i) Hx-mc-2, (j) Oc, (k) Oc-mc-1 and (l) Oc-mc-2.	32
2.23	Comparison between numerical and experimental values of SAE of specimens.	33
2.24	Metallic cylindrical shells as energy absorbers in automobile/train structures.	34
2.25	Final collapse modes of tempered aluminium tubes in (a) C2T4; (b) C7T6; (c) C2T3; (d) C6T6.	36
2.26	Final collapse modes of annealed aluminium tubes in (a) C2T4A; (b) C7T6A; (c) C2T3A; (d) C6T6A.	36
2.27	Comparison of the SEA of tempered and annealed aluminium tubes.	37
2.28	Typical engineering stress-strain curves.	38
2.29	Deformation modes of static tests.	39
2.3	Deformation modes of temper T4 under dynamic loading.	40
2.31	Deformation modes of temper T6 under dynamic loading.	40
2.32	Comparison between static and dynamic force displacement curves.	41

2.33	Schematic configuration of the steel square tube specimens: (a) without discontinuities (Type C), (b) with a hole at the middle height, (c) with a hole at 1/4 of height, (d) with a hole placed at 10 mm (or 7.5 mm) from the top and (e) with three holes at the preceding locations.	42
2.34	1 hole with diameter of 10mm in a distance from the top equal to the 1/4 of height.	43
2.35	1 hole with diameter of 10mm in a distance from the top equal to 10mm.	43
2.36	1 hole with diameter of 10mm in the middle height.	44
2.37	(a) views of progressive collapse (experimental), (b) views of progressive collapse (numerical simulation).	44
2.38	Effect of the aspect ratio of the initiators in the collapse of structures; (a) structure III-A, (b) structure III-F.	48
2.39	Test specimen configurations.	49
2.4	Photographs of the transient quasistatic crushing of specimen SA4_1.	51
2.41	Photographs of the transient quasistatic crushing of specimen SB5_H50_1.	52
2.42	Photographs of the transient quasistatic crushing of specimen SB8_HEq_1.	52
2.43	Arrangement of holes in cylindrical specimens.	53
2.44	Geometries of the energy absorbers with modifications .	56
2.45	Details of the selected energy absorber geometries .	57
2.46	Collapse modes for circular tubes under axial loading (a) ring mode; (b) diamond mode; (c) mixed mode .	58
2.47	Mode classification chart for circular aluminium tube .	58
2.48	Classification of the axial collapse of the cylindrical tube under quasi-static loading.	60
2.49	Typical crushing deformations of cylindrical tube. (a) Axisymmetric pattern (R=75 mm; H=2:0 mm; L=200 mm); (b) Non-axisymmetric pattern (R=75 mm; H=1:6 mm; L=250 mm); (c) Column buckling pattern (R=20 mm; H=3 mm; L=500 mm) .	61

2.5	Graph of absorbing energy versus R/H .	62
2.51	Graph of mean axial impact force versus RH2 .	62
2.52	Impact crushing deformation process of type 1 specimen. (a) Numerical simulation by DYNA3D.; (b) Experimental results .	64
2.53	A sample collapse model of grooved frusta tube .	64
2.54	Groove less specimens after axial crushing: (a) F0-6 and (b) E0-4 .	65
2.55	Grooved frusta specimens after axial crushing .	66
2.56	Different stage of buckling for specimens F0-6, F9-6, F15-6, and F17-6 .	67
2.57	Maximum crushing load vs. number of grooves .	67
3.1	Flow chart of the methodology.	69
3.2	Dimension of plate model	70
3.3	Geometry setup.	73
3.4	True stress and plastic strain data for Aluminium Alloy 6061-T6.	73
4.1	Comparison of internal energy and kinetic energy in a body.	76
4.2	Mesh convergence analysis.	77
4.3	Deformation shape and its respective force-displacement curve.	79
4.4	Comparison of energy absorbed for different geometry.	81
4.5	Comparison of specific energy absorption for different geometry.	81
4.6	Comparison of peak crushing force for different geometry.	82
4.7	Comparison of crushing force efficiency for different geometry.	83
4.8	Comparison of crushing strain for different geometry.	83
4.9	The location of the hole for Group 1.	85
4.1	The location of the hole for Group 2.	86
4.11	Deformation shape and its respective force-displacement curve for Group 1.	87
4.12	Deformation shape and its respective force-displacement curve for Group 2.	88
4.13	Comparison of the peak crushing force of the models.	89
4.14	Comparison of the mean crushing force of the models.	90
4.15	Comparison of the energy absorbed by the models.	90

4.16	Comparison of the specific energy absorbed by the models.	91
4.17	Comparison of crushing force efficiency of the models.	92
4.18	Comparison of the crushing strain of the models.	92



LIST OF TABLES

TABLE	TITLE	PAGE
2.1	The dimension of aluminium tube with their respective P_i , mean collapse load P_m and collapse mode under axial compression .	12
2.2	Force-displacement curve for all specimens under axial loading .	19
2.3	Mechanical properties of HSLA 350.	22
2.4	Comparison of FE model results and published results on 0.15 solidity .	23
2.5	Specifications and numerical result obtained for triangular tubes.	24
2.6	Specifications and numerical result obtained for square tubes.	24
2.7	Specifications and numerical result obtained for hexagonal tubes.	24
2.8	Specifications and numerical result obtained for octagonal tubes.	25
2.9	Specifications and numerical result obtained for circular tubes .	25
2.1	Specifications and numerical result obtained for square-multicell tubes .	25
2.11	Crushing load-deformation curve for different cross-section with solidity of 0.175 .	28
2.12	Mechanical properties of tempered and annealed aluminium alloys .	35
2.13	Coding of specimens .	35
2.14	Test programme.	38
2.15	Experimental and numerical results.	45
2.16	Specification for group I.	46
2.17	Specification for group II.	46
2.18	Specification for group III.	46
2.19	Result for group I.	47
2.2	Result for group II.	47
2.21	Result for group III.	47

2.22	Results for quasistatic axial crushing of square tubes with and without hole .	50
2.23	Comparison of performance parameters obtained from experiment.	55
2.24	FEA results for energy absorber geometries .	57
2.25	Dimension of the specimens .	63
2.26	Comparison between experimental results and FEM solutions .	63
2.27	Specimen dimensions .	65
3.1	Dimension of the shell model	71
3.2	Material properties of Aluminium Alloy 6061-T6.	73
4.1	Comparison of numerical and theoretical mean crushing force for three different shells.	80



LIST OF ABBREVIATION

Al	Aluminium
BIW	Body in white
CAD	Computer Aid Design
<i>CFE</i>	Crush force efficiency
Eq.	Equation
<i>EA</i>	Energy absorption
<i>SEA</i>	Specific energy absorption
<i>CS</i>	Crushing strain
MCF	Mean crushing force



LIST OF SYMBOLS

D	=	Outer diameter
F_{max}	=	Peak crushing force
F_{mean}	=	Mean crushing force
H	=	Folded length of plastic hinge
h	=	Height of the shell
m	=	Mass
S	=	Outer side length
t	=	Wall thickness of the shell
v	=	Velocity



CHAPTER 1

INTRODUCTION

1.1 Background

Thin-wall structure such as cylindrical shell has been widely applied in automotive, aerospace, petrochemical engineering, and marine because of the advantages of lightweight and high energy absorption structure. Cylindrical shell also having the advantages on its axisymmetric body which allow it to manufacture easily to increase their structure's ability (Tang et al., 2016).

Crashworthiness is the capacity for a structure or material to dissipate kinetic energy to deformation (Ghazali et al., 2017). In the automotive industry, crashworthiness is an important consideration to protect the occupant in the vehicle. As known, a greater time of impact can help in reducing injury on occupant from the impact (Bitesize, n.d.).

Crashworthiness can be affected by several factors such as the structure of the body and material selection. The structure of the body can be referring to the cross-section of the body whether it is in circle, triangular, or rectangular. Besides, the structure can be influence by changing its wall thickness.

On the other hand, the properties of the material can be a crucial factor for crashworthiness. Consideration of the ductility and the durability of the material based on the application purposes is important. An aluminium alloy having advantages in its lightweight properties, durability as well as corrosion resistance. These properties make it more reliable on the automotive industry application (Langseth et al., 1998).

1.2 Problem statement

In the automotive industry, crashworthiness is a crucial consideration to be focus on. Crashworthiness is strongly depending on the energy absorption capacity and the initial peak crushing force experienced by the structures. Even though cylindrical shell can absorb high amount of energy, it was found that the shell has experienced a relatively high amount of initial peak crushing force compared to others cross-section. This study analyses the crashworthiness of shells with different cross-sectional geometry and also the present of discontinuity.

1.3 Objectives

The objectives of this project are as follow:

- i. To study the deformation behaviour of the aluminium alloy shell with different cross-sectional geometry under quasi-static axial loading through Finite Element Analysis (FEA).
- ii. To investigate the energy absorption of aluminium alloy shell with different cross-sectional geometry subjected to quasi-static axial loading condition through FEA.
- iii. To identify the effect of discontinuity (hole) on the aluminium alloy shell towards crashworthiness of the shell.

1.4 Scope

This study focuses on finite element analysis using Abaqus 2020 to identify the crashworthiness of the thin-walled shells with various cross-sectional geometry (circle, square, and equilateral triangle). After identifying the shell with highest energy absorption capacity, the shell is modified (discontinuity) to improve its crashworthiness. All the shells will have the same cross-sectional area, wall thickness, and length. The material of the shells is assigned with aluminium alloy A6061. The shells will be subjected to quasi-static axial loading with a velocity of 5mm/min. The result from finite element analysis will be compared with the theoretical result.

CHAPTER 2

LITERATURE REVIEW

2.1 Introduction

This chapter cover the history of thin-walled structures and the implementation of thin-walled structures with axial loading. In addition, in order to interpret the effect of geometry and material properties, the respective results from the related analysis will be compared. The study also addressed the collapse behaviour of thin-walled structures subjected to axial loading by defining the collapse behaviour of the thin-walled structures. Moreover, the effect of discontinuity on the crashworthiness of the thin-walled shell is identified.

2.2 Thin-walled structures

Thin-walled structure has the advantages of being lightweight and, due to its ease of manufacturing, has a very low cost. These structures can be varying in different cross-section. For example, circular, square, triangular, polygonal, and conical. Moreover, these structures can be used individually or combined with polymeric and metallic foams to improve their crashworthiness (Nia and Hamedani, 2010). Thin-walled structures are widely used as kinetic energy absorbers as they are able to dissipate a large amount of kinetic energy through plastic deformation, cracking and fracture during a collision. Typical application of thin-walled structures such as the front rail and the front crossbeam in the car is used to dissipate the kinetic energy by longitudinal and transverse deformation. Longitudinal load

crash with higher energy absorption compared to transverse deformation. A lot of research is therefore carried out on the crashworthiness of thin-walled structures under axial crushing loading. (Tang et al., 2012).

Thin-walled structures such as plates and shells are the most common construction elements in nature and technology. This is independent of a specific scale. They can be small, such as cell membranes and tiny components of the system, or very large, such as airplane fuselages and cooling towers. A natural optimization technique for reducing dead load and decreasing the amount of construction material is this preference to apply walls as thin as possible. In shell structures, the beneficial effect of double curvature is used to optimally hold transverse loading, primarily by membrane forces having the opposite direction with bending moments (Bischoff et al., 2017). Very large deflections can be achieved through the deformation in plastic fold. This is important due to the number of plastic fold can influence the energy absorption capacity of the model. This is in stark contrast with the buckling or post-buckling behaviour of plates or shells in which slight disturbances contribute to a more or less uniform distribution of strain across a predominantly compressive state (Wierzbicki and Abramowicz, 1983).

Over the past years, crashworthiness research interests have resulted in a series of systematic investigations through theoretical, experimental and numerical approaches into crash responses of different thin-walled structures. Thin-walled components have shown considerable advantages compared with solid elements as thin-walled component sustain a relatively high load while maintain stable deformation, which may be substantially greater than the corresponding ultimate loads. One of the real-life example is the automobile body in white (BIW) which is mainly made up of a thin-walled component due to its high capability of absorbing energy performance and lightweight. (Sun et al., 2014). The most prevalent elements used as crash defence systems that transform kinetic energy into

irreversible plastic deformation energy are thin-walled tubular structures. These shock absorbers, with simple geometries, are light and can be easily attached to devices. The initial and gradual buckling of thin-walled tubes is caused by the compressive axial load. During axial crushing, the load variations decide the deceleration pulse during impact. (Ghamarian and Tahaye Abadi, 2011).

2.3 Crash Parameter

Crash parameters is the parameter that used to do comparison to differentiate the crashworthiness of the specimen. Some of the crash parameters are energy absorption (EA), mean crush force (F_{mean}), peak crush force (F_{max}), crush force efficiency (CFE), and specific energy absorption (SEA).

Generally, energy absorption, specific energy absorption, mean crushing force, the peak force, and the crash load efficiency are extensively used to measure the crashworthiness characteristics of thin-walled structures (Sofi, 2015). Different performance parameters such as EA , SEA , F_{mean} and F_{max} are used in order to investigate the energy absorption performance of thin-walled tubes. The parameters are obtained from their load-displacement responses (Baykasoglu, 2019).

The key to the modern dynamic design of structures is improved energy absorption along with a smooth load displacement curve, decreased peak force and high mean crushing force (Kamran et al., 2017). The ideal energy absorber would have a high value of EA , F_{mean} , and SEA while remaining a low value of F_{max} for the safety of the passenger. CFE should be maximized to fulfil all of these objectives. In addition, to eliminate damage to the automotive system, CS should be minimized (Davoudi and Kim, 2018; Tarlochan and Alkhatib, 2017).

2.3.1 Energy Absorption (EA)

The energy absorbed by the absorber can be determined by computing the work done by the crushing force. The total energy absorbed is the area under the force-displacement curve of the model. The total energy absorption can be expressed as in Eq. (2.1):

$$EA = \int_0^{\delta_{max}} F d\delta \quad (2.1)$$

where F is the axial load, δ is the displacement, and δ_{max} is the maximum displacement in the axial direction (Sofi, 2015; Tarlochan and Alkhatib, 2017; Davoudi and Kim, 2018; Baykasoglu, 2019; Li et al., 2021).

2.3.2 Mean crush force (F_{mean})

The mean crush force (F_{mean}) is the total energy absorption divided by the total crush displacement, as in Eq. (2.2). The high mean crush force for an element means a higher capability to absorb the crash energy (Sofi, 2015; Davoudi and Kim, 2018; Baykasoglu, 2019; Li et al., 2021).

$$F_{mean} = \frac{\int_0^{\delta_{max}} F d\delta}{\delta_{max}} \quad (2.2)$$

2.3.3 Peak crush force (F_{max})

The first peak load in the force-displacement curve is known as the Peak Crushing Force (PCF) (Kamran et al., 2017). The peak crushing force is the maximum force required for a structure to start plastic deformation. The consideration of this parameter is

importance as it is the force experienced by the occupant during the crash event (Tarlochan and Alkhatib, 2017). A higher peak crushing force may inflict damage to the body connected with it. Hence, it is crucial to achieving a low peak crushing force for a structure to be more crashworthiness (Davoudi and Kim, 2018).

2.3.4 Crush force efficiency (*CFE*)

The crushing force efficiency is the ratio of the mean crushing force to the peak crushing force (Sofi, 2015; Kamran et al., 2017), as in Eq. (2.3):

$$CFE = \frac{F_{mean}}{F_{max}} \quad (2.3)$$

A large value of *CFE* indicates an efficient energy absorption at the same time a low peak crushing force achieved (Davoudi and Kim, 2018; Li et al., 2021). The ideal energy absorber would preserve a peak load for its entire crushed length. A low *CFE* value will lead to a large deceleration shift and it will cause harm to the passenger (Tarlochan and Alkhatib, 2017).

2.3.5 Specific Energy Absorption (*SEA*)

The energy absorption per unit mass is a convenient measure for comparing the energy absorption capabilities of structures with different mass (Karagiozova and Jones, 2001). Specific Energy Absorption (*SEA*) is the ratio of dissipated energy to the total mass of the structure. It is the ratio of absorbed energy to the total mass of the structure (Kamran et al., 2017). The specific energy absorption (*SEA*) is the totally absorbed crash energy by the structure per unit mass, as expressed in Eq. (2.4):